

## Original paper

# Analysis of activity uptake, effective half-life and time-integrated activity for low- and high-risk papillary thyroid cancer patients treated with 1.11 GBq and 3.7 GBq of $^{131}\text{I}$ -NaI respectively



Pablo Mínguez<sup>a,b,\*</sup>, Emilia Rodeño<sup>c</sup>, José Genollá<sup>c</sup>, Maite Domínguez<sup>d</sup>, Amaia Expósito<sup>e</sup>, Katarina Sjögren Gleisner<sup>f</sup>

<sup>a</sup> Department of Medical Physics and Radiation Protection, Gurutzeta-Cruces University Hospital/Biocruces Health Research Institute, Barakaldo, Spain

<sup>b</sup> Faculty of Engineering, Department of Applied Physics I, UPV/EHU, Bilbao, Spain

<sup>c</sup> Department of Nuclear Medicine, Gurutzeta-Cruces University Hospital/Biocruces Health Research Institute, Barakaldo, Spain

<sup>d</sup> Department of General and Digestive Surgery, Basurto University Hospital, Bilbao, Spain

<sup>e</sup> Department of General and Digestive Surgery, Division of Endocrine Surgery, Basurto University Hospital, Bilbao, Spain

<sup>f</sup> Department of Medical Radiation Physics, Lund University, Lund, Sweden

## ARTICLE INFO

## Keywords:

Differentiated thyroid carcinoma

Thyroid remnants

$^{131}\text{I}$ -NaI activity

Pharmacokinetics

Dosimetry

## ABSTRACT

**Purpose:** To analyse the activity uptakes, effective half-lives and time-integrated activities, of relevance for remnant dosimetry, for patients treated for papillary thyroid cancer (PTC) with a different amount of activity of  $^{131}\text{I}$ -NaI.

**Methods:** Fifty patients were included. Of those, 18 patients had low-risk PTC and were treated with 1.11 GBq of  $^{131}\text{I}$ -NaI (Group 1), and 32 patients had high-risk PTC and were treated with 3.7 GBq (Group 2). Radioiodine was administered after total thyroidectomy and rTSH stimulation. Two SPECT/CT scans were performed for each patient to determine the remnant activities and effective half-lives.

**Results:** Significantly higher values ( $p < 0.05$ ) were obtained for Group 1 for the remnant activity at 7 d (medians 1.4 MBq vs 0.27 MBq), the remnant activity per administered activity at 2 d (0.35% vs 0.09%) and at 7 d (0.13% vs 0.007%), and the effective half-life (93 h vs 40 h). Likewise, the time-integrated activity coefficient was significantly higher for Group 1. The time-integrated activity did not differ significantly between the two groups ( $p > 0.05$ ).

**Conclusions:** We found a significant difference in the remnant activity per administered activity, the rate of washout from thyroid remnants, and the time-integrated activity coefficient between low-risk PTC patients treated with 1.11 GBq and high-risk PTC patients treated with 3.7 GBq. On the contrary, there was no such difference in the time-integrated activity. If remnant masses were also not statistically different (reasonable assumption for this monocentric study) no difference in time-integrated activity would imply no difference in remnant absorbed dose, of relevance for treatment efficacy and the risks of stochastic effects.

## 1. Introduction

The administration of  $^{131}\text{I}$ -NaI for the treatment of differentiated thyroid cancer (DTC) started in the 1940s [1,2] and still remains a reasonable option after surgery [3]. Iodide in blood is accumulated in thyroid tissue, where it is concentrated in thyroid follicular cells against an electrochemical gradient over the basal membrane via the sodium-iodide symporter (NIS). The basis of ablation is that the  $\beta^-$  particles

emitted by  $^{131}\text{I}$  cause acute thyroid-cell death [4].

The activity of  $^{131}\text{I}$ -NaI to administer in DTC treatments with ablative intent is usually empirically determined. Administered activities normally range between 1.11 GBq and 3.7 GBq [1,2], although higher values have been reported [5]. Based on the low amount of iodine present in therapeutic activities ( $< 1 \mu\text{g}$ ), the remnant absorbed dose has been assumed to be proportional to the administered activity [6]. However, it has also been reported that irradiation of thyroid cells

\* Corresponding author at: Department of Medical Physics and Radiation Protection, Gurutzeta plaza z/g, 48903 Barakaldo (Bizkaia), Spain.

E-mail addresses: [pablo.minguezgabina@osakidetza.eus](mailto:pablo.minguezgabina@osakidetza.eus) (P. Mínguez), [emilia.rodenoortizdezarate@osakidetza.eus](mailto:emilia.rodenoortizdezarate@osakidetza.eus) (E. Rodeño), [jose.genollasubirats@osakidetza.eus](mailto:jose.genollasubirats@osakidetza.eus) (J. Genollá), [maite.dominguezayala@osakidetza.eus](mailto:maite.dominguezayala@osakidetza.eus) (M. Domínguez), [amaia.expositorodriguez@osakidetza.eus](mailto:amaia.expositorodriguez@osakidetza.eus) (A. Expósito), [katarina.sjogren\\_gleisner@med.lu.se](mailto:katarina.sjogren_gleisner@med.lu.se) (K. Sjögren Gleisner).

<https://doi.org/10.1016/j.ejmp.2019.08.017>

Received 3 April 2019; Received in revised form 21 August 2019; Accepted 23 August 2019

Available online 29 August 2019

1120-1797/ © 2019 Associazione Italiana di Fisica Medica. Published by Elsevier Ltd. All rights reserved.

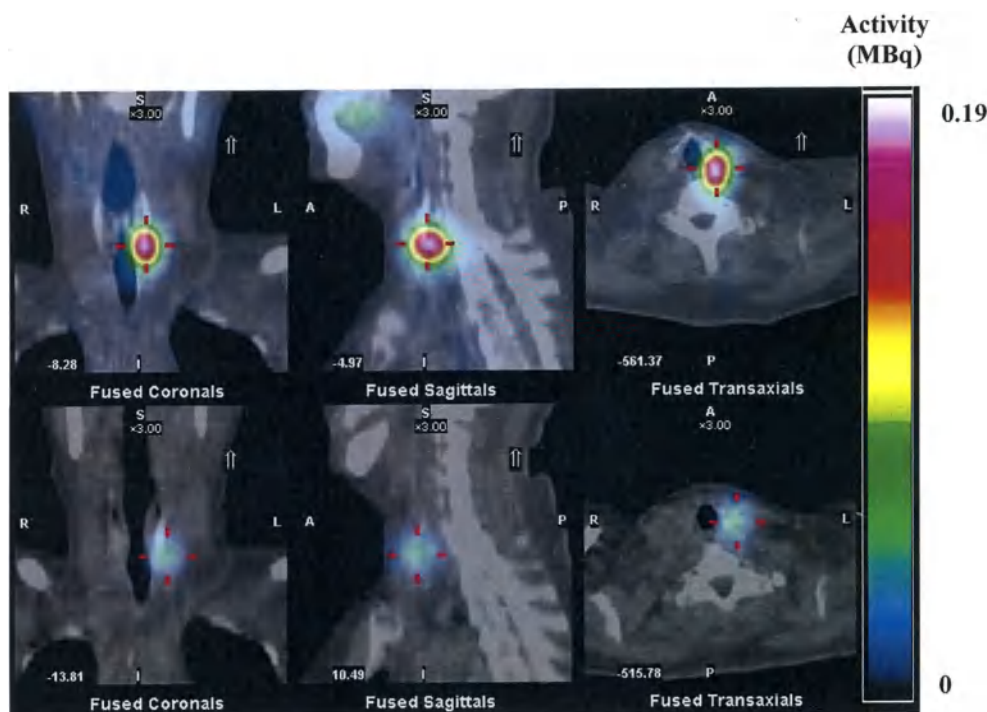


Fig. 1. Coronal, sagittal and transaxial reconstructed SPECT/CT images of the remnant of one patient. Images were acquired at 2 d (upper row) and 7 d (lower row) after administration.

during the early therapy phase may affect the radioiodine uptake (self-stunning effect) [7,8]. This, in turn, would mean that the remnant absorbed dose and the administered activity are not proportional. In particular, in [7] a reduced therapeutic uptake was observed for patients given tracers not only of  $^{131}\text{I-NaI}$ , but also of  $^{123}\text{I-NaI}$ , before treatment, and authors concluded that this reduction was attributable to the therapeutic activity itself during the early phase of therapy. In [8], a faster excretion was observed during therapy, in comparison to that observed after administration of a tracer, this pattern being more apparent in patients treated with the higher activities. However, given the limited amount of patients in these studies dealing with stunning [7,8], there is still need for more data to understand the uptake and washout of therapeutic administrations of  $^{131}\text{I-NaI}$ .

Thus, in order to investigate possible differences in the washout for patients treated with different activities, in this study we determined the remnant activity per administered activity, that is, the fractional radioiodine uptake, and the effective half-life of  $^{131}\text{I-NaI}$  in thyroid remnants for two groups of patients suffering from papillary thyroid cancer (PTC), and treated with a different amount of radioiodine activity (1.11 GBq vs 3.7 GBq). The administered activity was decided according to the clinical classification, where low-risk patients were treated with 1.11 GBq, while high-risk patients were treated with 3.7 GBq.

## 2. Materials and methods

### 2.1. Patient data and imaging

Fifty patients (41 female and nine male), aged between 24 and 73 years, treated for PTC were included. All patients underwent total thyroidectomy following the same surgical procedure, which was performed by the same group of surgeons. In none of the patients the cancer had spread to nearby tissues, lymph nodes or formed metastases. Following the analysis of the resected thyroid and lesion, patients were staged according to the UICC/AJCC TNM system [9]. Thus, patients with a lesion maximal diameter  $\leq 4$  cm were classified as low-risk PTC

and were treated with 1.11 GBq of  $^{131}\text{I-NaI}$  (Group 1), whereas those with a lesion maximal diameter  $> 4$  cm were classified as high-risk PTC and were treated with 3.7 GBq (Group 2). Of the 50 patients, there were 18 low-risk and 32 high-risk PTC patients. In approximately half of the patients of each group, more than one remnant with radioiodine uptake were identified in SPECT/CT images, and in total 81 remnants were analysed (28 in Group 1, and 53 in Group 2). In all cases, therapy was performed after stimulation with recombinant human thyroid stimulating hormone (rhTSH). On the day of treatment administration and before administering the radioiodine, plasma levels of thyroglobulin (Tg), free T4 and TSH were measured. After radioiodine administration, patients treated with 1.11 GBq remained as inpatients for 24 h, while patients treated with 3.7 GBq stayed for 48 h. Patients were released when the dose rate at 1 m was below  $40 \mu\text{Sv/h}$ , according to recommendations of the IAEA [10]. Institutional Ethics Committee approval was obtained, as well as informed consent from all patients.

Two SPECT/CT acquisitions centred on the neck region with automatic body contouring were performed for each patient. Imaging times were aimed to be at 2 d and 7 d after administration, although the time of the second acquisition for two patients was at 5 d, and for four patients at 6 d after administration, because of a lack of availability of the gamma camera. SPECT/CT acquisitions were performed employing a dual-head General Electric (GE, Fairfield, CT, USA) Infinia Hawkeye gamma camera, with a crystal thickness of 9.5 mm (3/8 in) and equipped with High-Energy General-Purpose collimators. A helical CT of pitch 1.9 and a duration time of 130 s was performed using 120 kVp (the lowest available value) and 2 mA. The CT was used for SPECT attenuation correction. SPECT projections were acquired in 60 angles, with 45 s per projection. A matrix size of  $128 \times 128$  was used, and a voxel size of  $0.442^3 \text{ cm}^3$ . A photopeak energy window centred at 364 keV and a width of 20% was used. For scatter correction a dual energy window method implemented by GE was employed, with an additional energy window centred at 297 keV and a width of 20%. SPECT image reconstruction was performed using the ordered subsets expectation maximisation (OSEM) algorithm in a Xeleris work station of GE, with 2 iterations and 10 subsets, applying a Butterworth filter

**Table 1**

Remnant activity at 2 d ( $A_2$ ), and 7 d ( $A_7$ ) after therapy administration, and remnant activity per administered activity at 2 d ( $A_2/A_{adm}$ ), and 7 d ( $A_7/A_{adm}$ ) after therapy administration, for Group 1 and Group 2. Data are presented as median (minimum, Q1, Q3, maximum). The  $p$ -value obtained from a Mann-Whitney  $U$  test is also shown.

	Group 1 ( $n = 28$ )	Group 2 ( $n = 53$ )	$p$ -value
$A_2$ (MBq)	3.9 ( $1.0 \times 10^{-1}$ , 1.2, 5.7, 33)	3.2 ( $5.2 \times 10^{-2}$ , 1.3, 7.3, 54)	0.92
$A_7$ (MBq)	1.4 ( $1.8 \times 10^{-2}$ , $6.2 \times 10^{-1}$ , 2.4, 18)	$2.7 \times 10^{-1}$ ( $5.3 \times 10^{-3}$ , $1.5 \times 10^{-1}$ , 1.0, 4.8)	< 0.05
$A_2/A_{adm}$ (%)	$3.5 \times 10^{-1}$ ( $9.0 \times 10^{-3}$ , $1.1 \times 10^{-1}$ , $5.2 \times 10^{-1}$ , 3.0)	$8.6 \times 10^{-2}$ ( $1.4 \times 10^{-3}$ , $3.5 \times 10^{-2}$ , $2.0 \times 10^{-1}$ , 1.5)	< 0.05
$A_7/A_{adm}$ (%)	$1.3 \times 10^{-1}$ ( $1.6 \times 10^{-3}$ , $5.6 \times 10^{-2}$ , $2.1 \times 10^{-1}$ , 1.7)	$7.2 \times 10^{-3}$ ( $1.4 \times 10^{-4}$ , $4.0 \times 10^{-3}$ , $2.7 \times 10^{-2}$ , $1.3 \times 10^{-1}$ )	< 0.05

with critical frequency 0.5 cycles/cm and power 10 (order 5). Analysis of SPECT images was performed using the ImageJ program [11]. The SPECT image full-width at half maximum (FWHM) of the point-spread function was determined by imaging a point source in air, and using the same acquisition and reconstruction parameters as for patients. The mean FWHM along the three principal axes of the gamma camera was obtained to 19 mm. Fig. 1 shows an example of patient SPECT/CT images corresponding to the two time points acquired.

## 2.2. Determination of activity, effective half-life and time-integrated activity

The remnant activity,  $A(t)$  was determined following a previously used method based on a thresholding technique [12]. A summary of the method is given in Appendix A. Since data were only available for two time points, and the estimated time-integrated activity can be sensitive to the method of integration, three different methods for calculation were applied, termed Methods I, II and III. The effective half-life was obtained from the two time points assuming a mono-exponential washout, as performed in previous studies [5,13,14]. For Method I, the time-integrated activity was calculated based on a model shown in [15] in which the uptake phase was approximated by a linear function of time from zero to the time of maximum uptake. This time was set to 1 d after administration, following the results in [16]. After 1 d the integration was performed following the assumed mono-exponential washout. For Method II, the integral from time zero to 1 d was instead approximated by a rectangular function, as earlier applied in [13,14]. For Method III, the uptake was assumed to occur instantly at time zero followed by a mono-exponential washout. Thus, the time-integrated activity was estimated according to

$$A = A_1 \left[ f + \frac{T}{\ln(2)} \right] \quad (1)$$

where  $A_1$  denotes the remnant activity at 1 d, and  $T$  is the effective half-life in unit of h. The factor  $f$  was set to  $f = 12$  for Method I,  $f = 24$  for Method II, and  $f = [T/\ln(2)] [2^{24/T} - 1]$  for Method III. The term  $A_1$  was determined by extrapolation from the remnant activity at 2 d using the effective half-life.

## 2.3. Statistical analysis

Differences between Group 1 and Group 2 were analysed for the clinically observed variables age, gender, levels of Tg, free T4 and TSH, the activity in the remnant at 2 d and 7 d after administration, as well as the remnant fraction of the administered activity at 2 d and 7 d. Differences in variables relevance for dosimetry were also analysed, including the effective half-life, the time-integrated activity, and the time-integrated activity coefficient (i.e. the time-integrated activity per administered activity also known as residence time).

The distributions of the continuous variables were tested for normality using the Shapiro-Wilks test, for which  $p < 0.05$  was considered non-normal. For variables that were normally distributed an independent samples  $t$ -test was performed, while for non-normally distributed variables a two-tailed Mann-Whitney  $U$  test was applied. For the categorical variable (gender) a chi-square test was performed. A

value of  $p < 0.05$  was considered significant. Statistical analyses were performed in the software R version 3.4.3 [17].

Descriptive analyses were made by boxplots, indicating the median value and lower and higher quartiles (Q1 and Q3). Whiskers were drawn based on the inter-quartile range (IQR = Q3–Q1), to indicate Q1 subtracted by 1.5 times the IQR, and Q3 added by 1.5 times the IQR. When these values were above the maximum value, or below the minimum value, whiskers were drawn at the maximum or minimum. Boxplots and correlation analyses were made in IDL (version 8.6, Harris Geospatial Solutions, Broomfield, Colorado, USA).

## 3. Results

### 3.1. Clinically observed variables

Except for the age, none of the variables studied followed a normal distribution. No significant differences were found in the age, gender, or levels of Tg, free T4 and TSH between Group 1 and Group 2 ( $p > 0.05$ ). Table 1 shows values of the remnant activity and the remnant activity per administered activity, in both cases at 2 d and 7 d after administration. For the six patients in whom the acquisition could not be performed at 7 d post administration, the activity at 7 d was determined by extrapolation using the effective half-life obtained from the available data points. Data are presented as median value (minimum, Q1, Q3, maximum). The obtained  $p$ -values obtained from the Mann-Whitney  $U$  test are also shown. Significant differences ( $p < 0.05$ ) between Group 1 and Group 2 were obtained for the remnant activity at 7 d after therapy administration, and the remnant activity per administered activity at 2 d and 7 d, but not in the remnant activity at 2 d. Fig. 2 shows boxplots, including the individual patient data underlying those summarised in Table 1. The asymmetry of the distributions is clearly seen.

### 3.2. Variables of relevance for dosimetry

Table 2 shows the results of the effective half-life, the time-integrated activity and the time-integrated activity coefficient. The obtained  $p$ -values obtained are also shown. Significant differences ( $p < 0.05$ ) between Group 1 and Group 2 were obtained for the effective half-life and the time-integrated activity coefficient but not for the time-integrated activity. Although the value of the time-integrated activity was dependent on the method used for integration, the presence/absence of statistically significant differences between patient groups did not change using different integration methods (Table 2). Fig. 3 shows boxplots of the effective half-life, the time-integrated activity, and the time-integrated activity coefficient, for Method I. As in Fig. 2 the asymmetry of the distributions can be noted.

## 4. Discussion

In the treatment of DTC, the pharmacokinetics of  $^{131}\text{I}$ -NaI is qualitatively known [18] but currently it cannot be quantitatively predicted for the individual patient. In this study, we examined clinical variables for low-risk PTC patients treated with 1.11 GBq (Group 1) and high-risk PTC patients treated with 3.7 GBq (Group 2). There were no significant

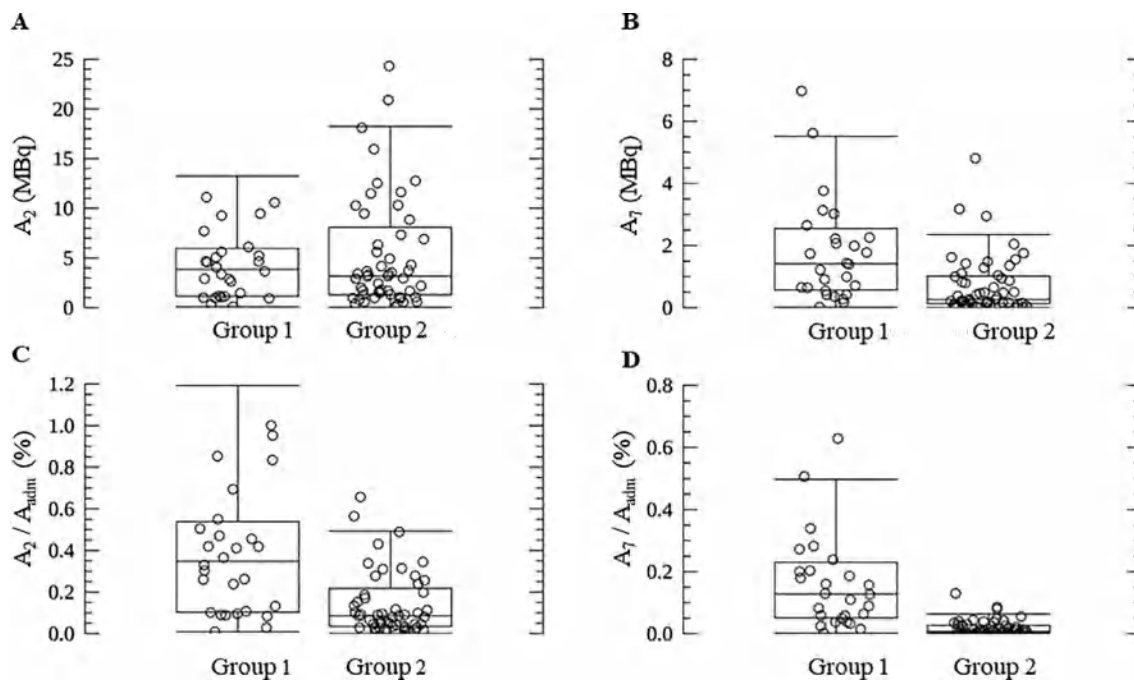


Fig. 2. Box plots of remnant activity at 2 d (A) and 7 d (B) after administration, and remnant activity per administered activity at 2 d (C) and 7 d (D). Symbols show individual patient values and have been randomly displaced in the horizontal direction for improved visibility.

differences in age, gender, the levels of Tg, free T4 or TSH between the two patient groups, and thus the subsequent statistical analyses were performed by only regarding the group, i.e. the administered activity combined with stage, as explanatory variable. The activity and patient stage could not be treated separately, due to the treatment protocol used.

As the most notable results (Figs. 2 and 3), the remnant activity at 7 d after administration was significantly lower ( $p < 0.05$ , Mann-Whitney  $U$  test) for Group 2 than for Group 1, and so was the effective half-life. When normalised to the administered activity, the remnant activity, that is, the fractional uptake, at both 2 d and 7 d was significantly lower for Group 2. This, in turn, yielded significantly lower time-integrated activity coefficients. The time-integrated activity did not differ significantly between the two groups, despite the different amounts of activities administered ( $p > 0.05$ , Mann-Whitney  $U$  test). From Figs. 2 and 3, the wide range of values obtained for patients in the respective group can also be noted. There are also other factors that may influence the radioiodine uptake and washout, such as the individual distribution volume, the remnant blood supply, and the renal clearance [19]. In this study, such variables were not available and could thus not be taken into account separately. For future studies, more detailed analyses would be warranted to better understand possible physiological and pharmacological reasons for the observed differences in the fractional uptake.

One may object to the limited number of imaging data points, at

approximately 2 d and 7 d, included in the current study. The time points were chosen for practical clinical reasons, and based on observed effective half-lives as deduced from the literature [5,12–14,20–22]. Recognising that the lack of an early time point data could potentially lead to erroneous time-integrated activities, three different methods were performed for integration of the early part of the curve. As noted in Table 2, the largest differences were obtained for Group 2, where the time-integrated activity calculated by Methods I and III differed by approximately 40%. In spite of these differences, the conclusions regarding the significance of the differences observed between Groups 1 and 2 did not change. In order to further verify the calculation of the time-integrated activity based on two data points, data from a previous study [12], in which acquisitions at 1 d, 2 d and 3 d-7 d were available, were reanalysed (Appendix B). A comparison of the time-integrated activity calculated using the current two-data point approach (Eq. (1), Method I) with that obtained using three time points is shown in Fig. 4. The limits of agreement (LOAs) were defined as 2 standard deviations around the mean difference, and were obtained to  $(-3.5 \pm 9.6) \%$ . Thus, there were no systematic differences between the methods based on two and three time points, and the LOAs were comparably narrow. However, the observed differences between patient Groups 1 and 2 are still significant, and are mainly governed by differences in the time-integrated activity, more specifically the activity uptake and the effective half-life.

Another drawback with the current study is related to limitations in

Table 2

Effective half-life ( $T$ ), time-integrated activity ( $A$ ) and time-integrated activity coefficient ( $a$ ) for Group 1 and Group 2. Data are presented as median (minimum, Q1, Q3, maximum). Methods I-III refer to the different time-activity integration methods (see text). The  $p$ -value obtained from a Mann-Whitney  $U$  test is also shown.

	Method	Group 1 ( $n = 28$ )	Group 2 ( $n = 53$ )	$p$ -value
$T$ (h)	N/A	93 (49, 78, 117, 172)	40 (13, 29, 58, 160)	< 0.05
$A$ (MBq h)	I	607 (12, 263, 1004, 8028)	343 (6, 149, 864, 5287)	0.13
	II	657 (13, 281, 1080, 8467)	425 (7, 172, 982, 6459)	0.20
	III	667 (14, 284, 1094, 8520)	491 (7, 181, 1029, 7272)	0.31
$a$ (h)	I	$5.5 \times 10^{-1}$ ( $1.1 \times 10^{-2}$ , $2.4 \times 10^{-1}$ , $9.0 \times 10^{-1}$ , 7.2)	$9.3 \times 10^{-2}$ ( $1.6 \times 10^{-3}$ , $4.0 \times 10^{-2}$ , $2.3 \times 10^{-1}$ , 1.4)	< 0.05
	II	$6.0 \times 10^{-1}$ ( $1.2 \times 10^{-2}$ , $2.6 \times 10^{-1}$ , $9.8 \times 10^{-1}$ , 7.7)	$1.2 \times 10^{-1}$ ( $1.8 \times 10^{-3}$ , $4.6 \times 10^{-2}$ , $2.7 \times 10^{-1}$ , 1.7)	< 0.05
	III	$6.1 \times 10^{-1}$ ( $1.3 \times 10^{-2}$ , $2.6 \times 10^{-1}$ , $9.9 \times 10^{-1}$ , 7.8)	$1.3 \times 10^{-1}$ ( $1.9 \times 10^{-3}$ , $4.9 \times 10^{-2}$ , $2.8 \times 10^{-1}$ , 2.0)	< 0.05

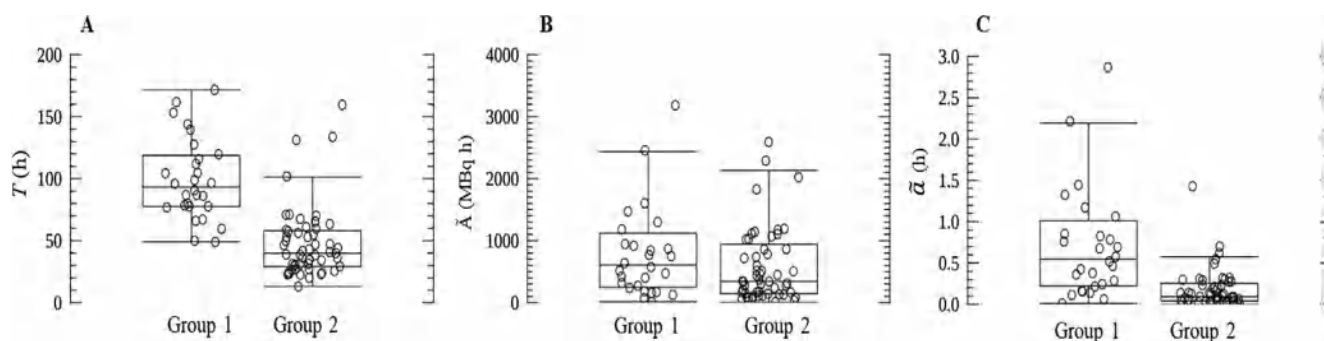


Fig. 3. Box plots of (A) effective half-life, (B) time-integrated activity and (C) time-integrated activity coefficient, i.e. the time-integrated activity normalized to the administered activity. Symbols show individual patient values and have been randomly displaced in the horizontal direction for improved visibility.

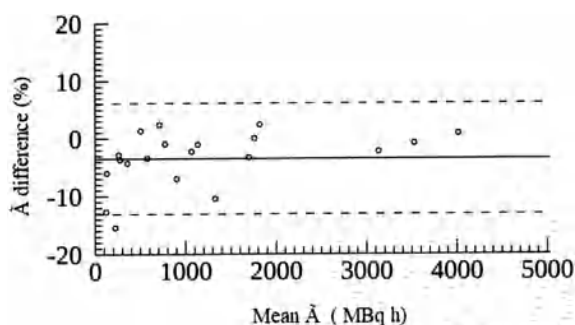


Fig. 4. The difference in time-integrated activity as a function of the mean time-integrated activity, for 20 thyroid remnants and two methods for its calculation, where data were retrieved from [12]. Time-integrated activity difference is calculated as  $(\bar{A}_2 - \text{point}) - \bar{A}_3 - \text{point}) / \bar{A}_3 - \text{point}$ . Solid line shows mean difference at  $-3.5\%$ , and dashed lines show the LOAs defined as 2 standard deviations around the mean.

the method used for tomographic reconstruction of SPECT images. Due to limitations in the clinical software used, the dual energy window method was used for scatter correction, and default values of the number of iterations and subsets of the OSEM reconstruction method. Improvements in the reconstruction software, such as the inclusion of the triple energy method for scatter correction would likely increase the accuracy of the estimated remnant activities. Likewise, an optimisation of the OSEM reconstruction method by increasing the number of iterations and subsets should contribute in the same direction [23]. Since thyroid remnants are not detectable in CT images, recovery coefficients for a segmentation based on the anatomic border were not applicable in this study. Thus, segmentation and recovery correction was performed using the previously developed thresholding method, described in Appendix A. The post-reconstruction filter applied is part of this method, and is used to suppress noise for the determination of the maximum-voxel count.

The lower effective half-lives observed for patients treated with 3.7 GBq seem to be consistent with the self-stunning effect reported in [7,8]. Hilditch et al. [7] compared the fractional uptake after a therapeutic activity of 4 GBq of  $^{131}\text{I}$ -NaI to the fractional uptake in DTC patients given diagnostic activities of 120 MBq of  $^{131}\text{I}$ -NaI (26 patients) or 200 MBq of  $^{123}\text{I}$ -NaI (16 patients). In all but one patient the fractional uptake was lower for the therapeutic than the diagnostic administration. Since a reduced therapeutic uptake was observed also for patients given  $^{123}\text{I}$ -NaI, authors concluded that this reduction was attributable to the therapeutic activity itself during the early phase of therapy. Sisson et al [8] hypothesized that stunning was a result of early effects of the therapeutic administration of  $^{131}\text{I}$ -NaI rather than the diagnostic activity, and tested this hypothesis by means of two sub studies. In the first sub study (70 patients) the impact of the amount of diagnostic  $^{131}\text{I}$  activity (18.5 MBq, 37 MBq and 74 MBq) on the therapeutic  $^{131}\text{I}$  uptake

was investigated. The fractional uptake at 2 d was lower for the therapeutic than for the diagnostic administration, but the amount of reduction was not correlated to the amount of diagnostic activity administered. In the second sub study (10 patients) the excretion pattern for  $^{131}\text{I}$ -NaI was investigated. Diagnostic  $^{131}\text{I}$  activities of 37 MBq, and therapeutic activities of 1.11 GBq (5 patients) and 5.55 GBq (5 patients) were administered, and the radioiodine uptake was measured at different time-points. A faster excretion was observed during therapy, this pattern being more apparent in patients treated with 5.55 GBq.

Although dosimetry is not part of the standard treatment setup, there are more studies that have reported on the effective half-lives [5,12–14,20–22]. In order to compare results from those studies, it has to be borne in mind that a lower effective half-life has been reported for patients treated after thyroid hormone withdrawal (THW) [19]. If studies that used rhTSH or THW are analysed separately, a trend of decreasing effective half-lives with higher administered activities can be noted, which could be explained again as a self-stunning effect. For instance for studies using rhTSH, mean effective half-lives of 117 h [12], 89 h [13] and 50 h [14] were reported for administered activities of 1.11 GBq, 3.0 GBq and 3.4 GBq, respectively. For studies using THW, mean effective half-lives of 112 h [5], 90 h [20] and 67 h [5] were reported for administered activities of 2.0 GBq, 3.0 GBq and 3.4 GBq, respectively.

Several studies have made ambiguous conclusions as to whether a higher activity results in better treatment outcomes than a lower one [24–29]. Considering that some studies have reported a correlation between the remnant absorbed dose and the success of remnant ablation [13,21,30], it may be hypothesised that the time-integrated activity, which represents the total number of decays in the remnant, plays a relevant role in the treatment outcome. Considering that for our patient data the time-integrated activities were not significantly different for patients given 1.11 GBq and for those given 3.7 GBq, the results from this study can be thus seen as hypothesis generating. In themselves, our data are not sufficient to test the hypothesis that the amount of activity has an effect on the effective half-life, as the patient stage and activity level could not be treated separately. This hypothesis would have to be tested in clinical studies including patients at different stages who were randomised to treatment with different activity levels, and where dosimetry is included in the treatment protocol. The possibility to decrease the administered activity is worth attention, considering that it would entail a shorter in-patient period and a lower risk of stochastic effects for patients.

## 5. Conclusions

In thyroid remnant treatment with ablative intention, patients treated with 3.7 GBq of  $^{131}\text{I}$ -NaI for high-risk PTC showed a significantly lower effective half-life and fractional uptake at 2 d and 7 d ( $p < 0.05$ , Mann-Whitney  $U$  test) than those treated with 1.11 GBq for low-risk PTC. The time-integrated activity did not differ significantly

between the two groups, despite the different amounts of activities administered ( $p > 0.05$ , Mann-Whitney  $U$  test). If, for this monocentric study, the assumption is made that remnant masses were also not statistically different, no difference in time-integrated activity would imply no difference in absorbed dose. In other words, owing to different kinetics, it is possible that administration of 1.11 GBq is as effective as 3.7 GBq for remnant ablation, with lower risks for stochastic effects and more convenient logistics as a consequence.

#### Declaration of Competing Interest

The authors declare that they have no known competing financial

#### Appendix A. Determination of the remnant activity

The method used for quantification of the remnant activity was identical to the one termed “Whole-volume dosimetry (Method 1)” in [12]. Briefly, the method was based on SPECT/CT imaging of the IEC-Standard 61675-1 image-quality phantom, containing six  $^{131}\text{I}$ -filled spheres in a cold background with volumes between  $0.5\text{ cm}^3$  and  $26.5\text{ cm}^3$ , and activities between 1.2 MBq and 10.6 MBq. During evaluation it was observed that a 5%-threshold applied to a region surrounding each sphere yielded an estimate of the activity to within 10%. It was also observed that the ratio of counts,  $f_{30}$ , obtained with 30%-threshold and 5%-threshold was approximately constant over the sphere volume. The remnant counts in patients was thus determined by first applying a 30%-threshold to avoid the inclusion of counts from activity in surrounding tissues, and then applying the predetermined counts ratio  $f_{30}$ . The resulting number of counts was then converted to activity by application of a calibration factor determined by SPECT imaging of a large cylindrical phantom with a homogenous solution of  $^{131}\text{I}$ . Please see [12] for details.

#### Appendix B. Analysis of the effect of acquiring a time point at 1 d on the time-integrated activity

The method for estimation of the time-integrated activity by Method I in Eq. (1) was investigated based on data acquired during a previously published study [12], which was focused on dosimetry in 20 thyroid remnants in 18 patients treated with  $^{131}\text{I}$ -NaI. In that study SPECT/CT was performed at 1 d, 2 d, and 3 d–7 d after administration. Activity quantification was performed following the same method as in the current study. In order to analyse the influence of acquiring a time point at 1 d, two methods were used for determination of the time-integrated activity; the 2-point method (Eq. (1), Method I) applied to data from 2 d and 3 d–7 d, and also a three-point method based on all three data points. For the three-point method, a combination of trapezoid and analytical integration was used, according to:

$$\tilde{A}_1 = A_1 \cdot t_1 / 2 \quad (\text{B1})$$

$$\tilde{A}_2 = (A_1 + A_2) / 2 \cdot (t_2 - t_1) \quad (\text{B2})$$

$$\tilde{A}_3 = A_2 / \lambda \quad (\text{B3})$$

$$\tilde{A} = \tilde{A}_1 + \tilde{A}_2 + \tilde{A}_3 \quad (\text{B4})$$

where  $A_1$ ,  $A_2$ , and  $A_3$  are the activities at the corresponding time points  $t_1$ ,  $t_2$ , and  $t_3$  (i.e. at approximately 1 d, 2 d, and 3 d–7 d after administration), and  $\lambda$  is the effective decay calculated from the data at 2 d and 3 d–7 d. Eq. B(1) thus represents a linear uptake from the time of administration until 1 d, while Eq. B(3) represents the washout after 2 d. The time-integrated activity obtained from the three-point method was compared to results from Eq. (1), applied to the same set of patient data, using Bland–Altman analysis (see Section 4).

#### References

- [1] Silberstein EB, Alavi A, Balon HR, et al. The SNMMI practice guideline for therapy of thyroid disease with  $^{131}\text{I}$  3.0. *J Nucl Med* 2012;53:1633–51.
- [2] Luster M, Clarke SE, Dietlein M, et al. Guidelines for radioiodine therapy of differentiated thyroid cancer. *Eur J Nucl Med Mol Imaging* 2008;35:1941–59.
- [3] Clerc J, Verburg FA, Avram AM, et al. Radioiodine treatment after surgery for differentiated thyroid cancer: a reasonable option. *Eur J Nucl Med Mol Imaging* 2017;44:918–25.
- [4] McDougall IR. Management of thyroid cancer and related nodular disease. London: Springer-Verlag; 2006.
- [5] Samuel AM, Rajashekhara B. Radioiodine therapy for well-differentiated thyroid cancer: a quantitative dosimetric evaluation for remnant thyroid ablation after surgery. *J Nucl Med* 1994;35:1944–50.
- [6] Walrand S, Hesse M, Jamar F. Statistical and radiobiological analysis of the so-called thyroid stunning. *EJNMMI Res* 2015;5:67. <https://doi.org/10.1186/s13550-015-0144-9>.
- [7] Hilditch TE, Dempsey MF, Bolster AA, et al. Self-stunning in thyroid ablation: evidence from comparative studies of diagnostic  $^{131}\text{I}$  and  $^{123}\text{I}$ . *Eur J Nucl Med* 2002;29:783–8. <https://doi.org/10.1007/s00259-002-0785-6>.
- [8] Sisson JC, Avram AM, Lawson SA, et al. The so-called stunning of thyroid. *J Nucl Med* 2006;47:1406–12.
- [9] Sobin LH, Gospodarowicz MK, Wittekind C. TNM classification of malignant tumors. 7th ed. New York: Wiley-Blackwell; 2009.
- [10] International Atomic Energy Agency. Release of patients after radionuclide therapy. Safety Report Series No. 63, IAEA. Vienna. 2009.
- [11] Rasband WS, ImageJ, U. S. National Institutes of Health, Bethesda, Maryland, USA, <https://imagej.nih.gov/ij/>, 1997–2016.
- [12] Mínguez P, Flux G, Genollá J, et al. Whole-remnant and maximum-voxel SPECT/CT dosimetry in  $^{131}\text{I}$ -NaI treatments of differentiated thyroid cancer. *Med Phys* 2016;43:5279–87.
- [13] Flux GD, Haq M, Chittenden SJ, et al. A dose-effect correlation for radioiodine ablation in differentiated thyroid cancer. *Eur J Nucl Med Mol Imaging* 2010;37:270–5.
- [14] Lassmann M, Luster M, Hanscheid H, et al. Impact of  $^{131}\text{I}$  diagnostic activities on the biokinetics of thyroid remnants. *J Nucl Med* 2004;45:619–25.
- [15] Jentzen W, Freudenberg L, Eising EG, et al. Optimized  $^{124}\text{I}$  PET dosimetry protocol for radioiodine therapy of differentiated thyroid cancer. *J Nucl Med* 2008;49(6):1017–23.
- [16] Gulec SA, Kuker RA, Goryawala M, et al.  $^{124}\text{I}$  PET/CT in patients with differentiated thyroid cancer: clinical and quantitative image analysis. *Thyroid* 2016;26(3):441–8.
- [17] R Core Team (2014). R: A language and environment for statistical computing. R Foundation for Statistical Computing, Vienna, Austria. URL <http://www.R-project.org/>. 2014.
- [18] Nyström E, Berg GEB, Jansson SKG, et al. Thyroid disease in adults. Berlin Heidelberg: Springer-Verlag; 2011.
- [19] Hanscheid H, Lassmann M, Luster M, et al. Iodine biokinetics and dosimetry in radioiodine therapy of thyroid cancer: procedures and results of a prospective international controlled study of ablation after rhTSH or hormone withdrawal. *J Nucl Med* 2006;47:648–54.
- [20] O’Connell MEA, Flower MA, Hinton PJ, et al. Radiation-dose assessment in radioiodine therapy—doseresponse relationships in differentiated thyroid-carcinoma

- using quantitative scanning and PET. *Radiother Oncol* 1993;28(1):16–26.
- [21] Maxon HR, Thomas SR, Hertzberg VS, et al. Relation between effective radiation dose and outcome of radioiodine therapy for thyroid cancer. *N Engl J Med* 1983;309:937–41.
- [22] Maxon 3rd HR, Englaro EE, Thomas SR, et al. Radioiodine-131 therapy for well-differentiated thyroid cancer—a quantitative radiation dosimetric approach: outcome and validation in 85 patients. *J Nucl Med* 1992;33:1132–6.
- [23] Dewaraja Y, Ljungberg M, Green AJ, et al. MIRDOSE pamphlet No. 24: guidelines for quantitative <sup>131</sup>I SPECT in dosimetry applications. *J Nucl Med* 2013;54(2):2182–8.
- [24] Hackshaw A, Harmer C, Mallick U, et al. <sup>131</sup>I activity for remnant ablation in patients with differentiated thyroid cancer: a systematic review. *J Clin Endocrinol Metab* 2007;92:28–38.
- [25] Mäenpää HO, Heikkonen J, Vaalavirta L, et al. Low vs. high radioiodine activity to ablate the thyroid after thyroidectomy for cancer: a randomized study. *PLoS ONE* 2008;3(4):e1885 <https://doi.org/10.1371/journal.pone.0001885>.
- [26] Mallick U, Harmer C, Yap B, et al. Ablation with low-dose radioiodine and thyrotropin alfa in thyroid cancer. *N Engl J Med* 2012;366(18):1674–85.
- [27] Castagna MG, Cevenini G, Theodoropoulou A, et al. Post-surgical thyroid ablation with low or high radioiodine activities results in similar outcomes in intermediate risk differentiated thyroid cancer patients. *Eur J Endocrinol* 2013;169(1):23–9.
- [28] Cheng W, Ma C, Fu H, et al. Low- or high-dose radioiodine remnant ablation for differentiated thyroid carcinoma: a meta-analysis. *J Clin Endocrinol Metab* 2013;98(4):1353–60.
- [29] Valachis A, Nearchou A. High versus low radioiodine activity in patients with differentiated thyroid cancer: a meta-analysis. *Acta Oncol* 2013;52(6):1055–61.
- [30] Wierts R, Brans B, Havekes B, et al. Dose-response relationship in differentiated thyroid cancer patients undergoing radioiodine treatment assessed by means of <sup>124</sup>I PET/CT. *J Nucl Med* 2016;57(7):1027–32.